Electric Modulus and Polarization Studies on Piezoelectric Polyimides

Beatriz Gonzalo,[1] Jose Luis Vilas,[2] María San Sebastián,[2] Tomasz Breczewski,[3] Miguel Ángel Pérez-Jubindo,[3] María Rosario de la Fuente,[3] Matilde Rodríguez,[2] Luis Manuel León[2]

[1]*GAIKER Technology Centre, Parque Tecnológico de Zamudio, Edificio 202, 48170 Zamudio, Spain*
[2]*Departamento de Química-Física, Facultad de Ciencia y Tecnología, Universidad del País Vasco, Apdo. 644, 48080 Bilbao, Spain*
[3]*Departamento de Física Aplicada II, Facultad de Ciencia y Tecnología, Universidad del País Vasco, Apdo. 644, 48080 Bilbao, Spain*

Received 3 November 2010; accepted 18 April 2011
DOI 10.1002/app.34702
Published online 16 December 2011 in Wiley Online Library (wileyonlinelibrary.com).

ABSTRACT: The piezoelectric polymeric sensors and actuators are widely valued because of their low density, availability to obtain complex shapes, and easy processing among other characteristics. However, there are not many useful piezoelectric polymers. Aromatic polyimides are high-performance polymeric materials characterized by thermal stability, chemical resistance, and excellent mechanical properties. Besides, some of these polymers have been reported as candidates to present piezoelectric properties. Our research focuses in the electric characterization of three piezoelectric amorphous aromatic polyimides, containing CN groups in different number and positions. The piezoelectricity in amorphous polymers is mainly due to the orientation polarization of the molecular dipoles, which is induced by the application of an external electrical field to a temperature over their glass transition temperature (T_g). Polyimides are measured by thermally stimulated depolarization currents and dielectric spectroscopy and the analysis of the dielectric data has been performed using the electric modulus formalism to separate conductive and dipolar processes. These measurements have evidenced that the frozen-in polarization is mainly due to the dipole orientation of the dipolar CN groups, allowing us to understand in depth the mechanism of polarization that contributes to the piezoelectric properties. This will facilitate the obtention of materials with the best possible piezoelectric properties, comparable to those currently available but with higher mechanical and thermal performance. © 2011 Wiley Periodicals, Inc. J Appl Polym Sci 125: 67–76, 2012

Key words: polyimides; frozen-in polarization; dielectric properties

INTRODUCTION

In the last decades, different amorphous polymers have been extensively investigated due to their piezoelectric and pyroelectric properties. However, a polymer that fulfils all market demands as high piezoelectric response and stability at high temperatures has not been found yet. Most commonly used polymers are substituted with nitrile groups such as polyacrylonitrile (PAN),[1] poly(vinyl acetate of vinylidene cyanide) (PVDCN/VAc),[2] or polyphenylethernitrile (PPEN).[3] Although these materials exhibit piezoelectricity, they have important disadvantages such as low glass transition temperature and humidity absorption that limit their use. In the last years[4–6] polyimides have emerged as the most promising amorphous piezoelectric polymers because of their good thermal stability (high glass transition and initial degradation temperatures), as well as excellent mechanical and dielectric properties. In addition, their piezoelectric properties can be improved adding pendant highly polar groups in the repetition unit owing to the ease with which may be placed upon it. Apart from being used as piezoelectric and pyroelectric materials, polyimides have many more applications, for example, as flexible insulators in electronics or for thermal garments.[7]

To produce a piezoelectric material from an amorphous polar polymer, the material should be poled by applying a strong electric field, E_p, at a temperature higher than its glass transition temperature, T_g.[8] The obtained frozen-in polarization, P_r, is given by:[9]

$$P_r = \varepsilon_0 \Delta\varepsilon_\alpha E_p, \quad (1)$$

where ε_0 is the permittivity of free space and $\Delta\varepsilon_\alpha = \varepsilon_S - \varepsilon_\infty$ the dipolar dielectric relaxation strength. ε_S

Correspondence to: Luis Manuel León (luismanuel.leon@ehu.es).

Contract grant sponsor: ETORTEK (Technology Centres Foundation Iñaki Goenaga, project ACTIMAT).
Contract grant sponsor: Spanish Government (project MICINN); contract grant number: MAT 2009-14636-C03-02.
Contract grant sponsor: Basque Government; contract grant number: project GIC10/45.

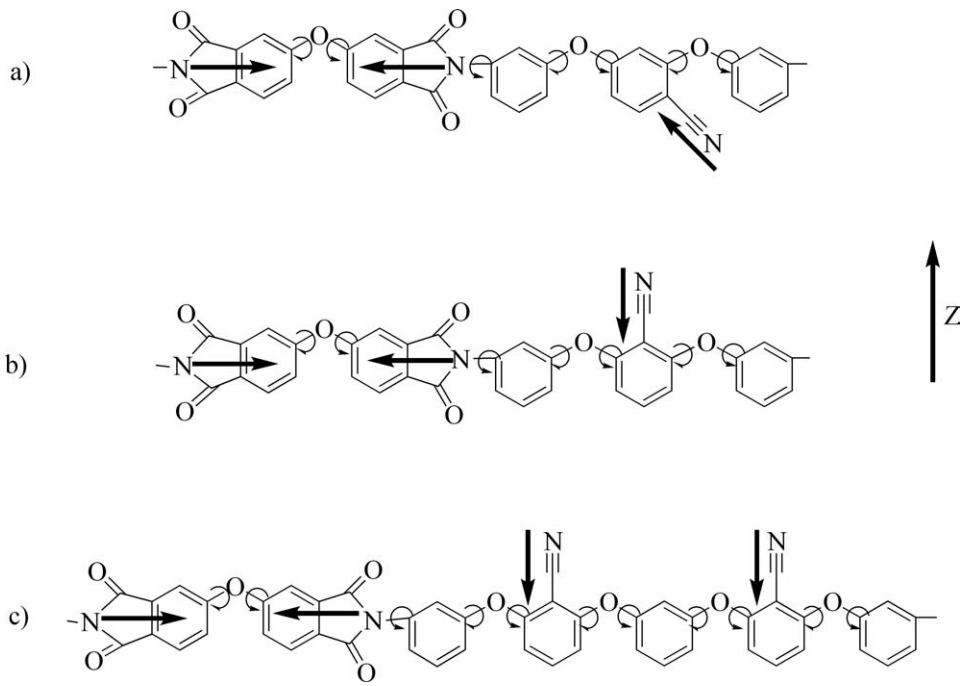

Figure 1 Chemical structure of the polyimides including the most important dipolar moments: a) poly2-4, b) poly2-6, and c) poly2CN.

and ε_∞ stand for the limiting low and high frequency permittivities with respect to the entire dielectric dispersion region that arises from the reorientational motions of the dipolar molecules. For amorphous polymers, there is a linear relationship between $\Delta\varepsilon_\alpha$ and the piezoelectric response:

$$d_h = -(\beta/3)\varepsilon_\infty P_r = -(\beta/3)\Delta\varepsilon_\alpha\varepsilon_0\varepsilon_\infty E_p, \qquad (2)$$

where d_h is the hydrostatic piezoelectric strain constant and β the volume compressibility. Once the piezoelectric response is directly proportional to P_r, β and $\Delta\varepsilon_\alpha$,[8] these values should be maximized, for example, by a more efficient grade of dipole alignment during the poling process and/or increasing the number of dipole groups in the repetitive unit of the polymeric chain.

The aim of our work was to study the dielectric properties (dielectric permittivity and frozen-in polarization) of three polyimides with differences in the position as well as the number of dipolar CN groups in the repetitive unit of the polymeric chain.

EXPERIMENTAL

Sample preparation

The synthesis and preliminary characterization of the three polyimides object of the present work, poly2-4, poly2-6, and poly2CN have been previously published.[10] Their chemical structure is shown in Figure 1. They are the result of a stoichiometric reaction between a commercial dianhydride, 4,4′-anhydride oxydiphthalic, and the corresponding diamine, 2,4-di(3-aminophenoxy)benzonitrile, 2,6-*bis*(3-aminophenoxy)benzonitrile, and 1,3-*bis*[2-cyano-3-(3-aminophenoxy)phenoxy]benzene, respectively. After obtaining the polyamic acids further thermal treatment produces the polyimides.

Films were prepared by dissolving the polyamic acid(s) in *N,N*-dimethylacetamide and evaporating at a sufficiently low rate to avoid bubble formation (curing step). The glass transition temperatures of these films, determined by differential scanning calorimetry (DSC), were 469 K for poly2-4, 473 K for poly2-6, and 449 K for poly2CN. The initial degradation temperature was higher than 700 K for the three polymides.[10] The curing temperatures for the polyamic acids were 483 K for poly2-4, 493 K for poly2-6, and 473 K for poly2CN. The resulting films were rectangular, their size being 50 × 25 mm^2 and 240 μm thick.

Dielectric spectroscopy

The complex dielectric permittivity, $\varepsilon^*(\omega) = \varepsilon'(\omega) - j\varepsilon''(\omega)$, was measured for nonpolarized samples over the frequency range 10^{-1} to 10^6 Hz using a Schlumberger 1260 frequency response analyzer accomplished with a high-impedance preamplifier of variable gain BDC from Novocontrol. The cell contained two 5-mm (diameter) gold plated electrodes separated by the polymer as dielectric, resulting in a parallel plate capacitor located at the end of a coaxial

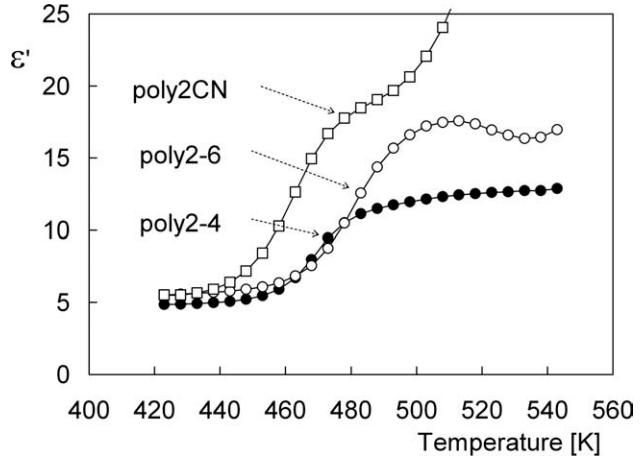

Figure 2 Temperature dependence of the real component of the complex dielectric permittivity, ε′, at 10 Hz, for poly2-4, poly2-6, and poly2CN.

line. A modified HP16091A coaxial test fixture was used as the sample holder. It was held in a cryostat from Novocontrol, which screens the system, and both temperature and dielectric measurements were computer controlled. The measurements were performed on cooling from 543 K (533 K for poly2CN) to room temperature with stabilization at each 5 K with a temperature control of 0.1 K.

Thermally stimulated depolarization current (TSDC) measurements

Cylindrical films of 6 mm diameter were polarized by the positive corona poling method. A dc voltage of 7 kV was applied using a HiTek Power Series 4000 as the supply source, being the tip placed at 10 mm from the sample. The temperature was raised up to $(T_g + 10)$ K at a rate of 2 K min^{-1}. The samples were kept during 1 h at this temperature. Then the temperature was decreased to room temperature at 5 K min^{-1} while the electric field was on, to freeze the polarized state.

The frozen-in polarization, P_r, of the poled samples was measured by the thermally stimulated depolarization current (TSDC) method.[11] The short-circuit current created as a result of the depolarization of the polymer sample with the increase of temperature was measured by a Keithley 6517 electrometer. The sample was heated in a thermostat (THMSE 600 from Linkam), at a constant rate of 1 K min^{-1}, from room temperature up to 523 K. The value of the frozen-in polarization, P_r, was obtained by integrating the current $i(T)$ with respect to time (temperature)

$$P_r = \frac{q}{A} = \frac{1}{A}\int_{t_0}^{t} i(t)dt = \frac{1}{Av}\int_{T_0}^{T} i(T)dt \qquad (3)$$

where q is the depolarization charge, A the electrode area, v the heating rate, and T_0 and T the initial and final temperatures.

RESULTS AND DISCUSSION

Dielectric permittivity measurements

Figure 2 shows the temperature dependence of ε′ at 10 Hz for the three polymers. Data were obtained under isothermal conditions, all three polymers exhibited similar behavior. As the temperature increased, from room temperature up to 420 K, the values of ε′ were practically kept stable. In general, amorphous polyimides exhibit the so called β or secondary relaxation in this temperature range below the glass transition,[12,13] that in our case did not seem to be present. Above the glass transition temperature, the dielectric permittivity exhibits a sharp increase being this jump related to the increase in mobility. This contribution is the so-called α relaxation. It happens at temperatures close to the calorimetric glass transition temperature. However, the permittivity value was greatly affected, as we will show later, by the conductivity, which, for example, made it very difficult to determine the associated dielectric strength directly from these measurements.

As an example representative of the three polyimides, in Figure 3 we have plotted ε′ versus temperature at several frequencies for poly2-6. The increase of ε′ as the frequency decreases indicated the presence of the above-mentioned α relaxation process. However, it is masked by another contribution related to the electric conductivity, clearly evidenced for high temperatures and low frequencies. The presence of an important electric conductivity above the glass transition temperature is observed in many polymers.[14] This fact is usually associated with the generation and transport of polarization-induced

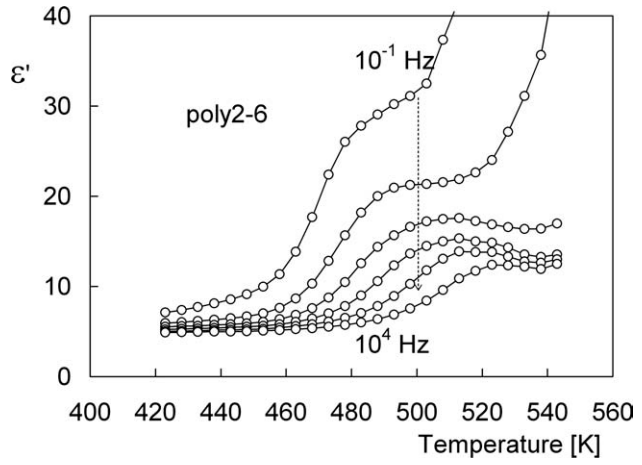

Figure 3 Temperature dependence of ε′ at different frequencies for poly2-6.

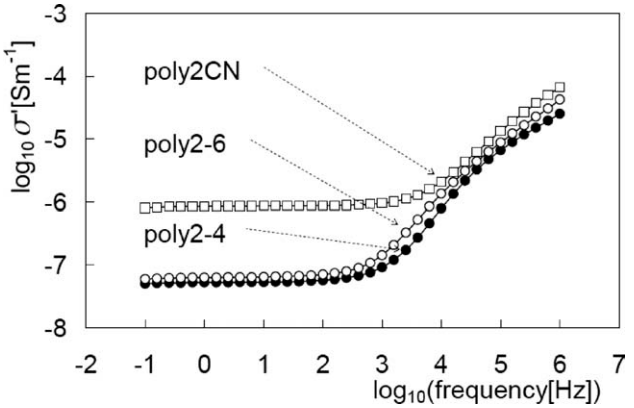

Figure 4 Log-log plot of the electric conductivity, σ′, versus frequency at T_g + 45 K for poly2-4, poly2-6, and poly2CN.

charges through the polymer matrix under the action of an electric field and appears as an undesirable low-frequency increase in both ε′ and ε″.[15,16] One of the aims of our work was to separate and discriminate both contributions. First, we needed to analyze this effect in terms of the real part of the complex conductivity, σ*(ω), related to the complex permittivity by:

$$\sigma^*(\omega) = \sigma'(\omega) - j\sigma''(\omega) = j\omega\varepsilon_0\varepsilon^*(\omega). \tag{4}$$

Figure 4 shows the real part of the conductivity, σ′, versus frequency in a log-log plot for the three polyimides at T_g + 45 K. On the low frequency side a plateau is observed, which can be extrapolated to the dc conductivity σ_0. At higher frequencies dispersion in σ′ is observed; this magnitude increases strongly with frequency. This behavior is quite universal and in absence of dipolar relaxations the following expression is usually assumed[17,18]:

$$\sigma'(\omega) = \sigma_0(1 + (\omega\tau)^s), \tag{5}$$

where s ranges between 0 and 1 and τ plays the role of a relaxation time for the conductivity. However, this expression lacks any theoretical foundation.[19] This plot evidences for example that poly2CN exhibits its higher conductivity level than poly2-4 and poly2-6. At high frequency, more evident for lower temperatures, the deviation from this power law indicates the presence of the α relaxation process. For those cases in which there is a dipolar relaxation process associated with an important conductivity contribution it is more convenient to analyze the dielectric spectra using the electric modulus formalism pioneered by McCrum et al.[20] and Macedo et al.[18] The complex electric modulus, $M^*(\omega)$, defined as the inverse of the complex dielectric permittivity:

$$M^*(\omega) = 1/\varepsilon^*(\omega) = M'(\omega) + jM''(\omega) \tag{6}$$

can be resolved into real and imaginary parts in terms of ε′ and ε″; as:

$$M'(\omega) = \frac{\varepsilon'(\omega)}{\varepsilon'^2(\omega) + \varepsilon''^2(\omega)}, \tag{7a}$$

$$M''(\omega) = \frac{\varepsilon''(\omega)}{\varepsilon'^2(\omega) + \varepsilon''^2(\omega)}. \tag{7b}$$

This formalism has been successfully applied to evaluate conductivity effects in polymers like polyethylene terephthalate,[21,22] nylon-11,[23,24] polyether imide,[25] and segmented polyurethanes.[26–28] However, as we will show later, this representation is very useful in our case because it allows us to discriminate between conductive and dipolar relaxation better than in other representations, based on the greater weight of the high frequencies for the modulus.[19]

Figure 5 shows three-dimensional plots of the imaginary part of the electric modulus, M'', versus temperature and frequency for (a) poly2-4, (b) poly2-6, and (c) poly2CN, from experimental results. Two thermally activated relaxation processes can be clearly observed. The one that appears at the isothermal condition in the low frequency region is associated with the conductivity phenomenon, σ relaxation process, also observable when representing σ′, as we have seen before (see Fig. 4). Relaxation at higher frequencies and at temperatures close to the respective glass transition temperature is associated with the dipolar α relaxation.

Let us analyze these spectra in detail. For each temperature above the glass transition the results were fitted to a sum of two Havriliak-Negami terms,[29] one for the conductivity (labeled by σ) and another for the α process (labeled by α):

$$M^*(\omega) = M_\infty + \frac{\Delta M_\sigma}{(1 + (j\omega\tau_{M,\sigma})^{\beta_1})^{\gamma_1}} + \frac{\Delta M_\alpha}{(1 + (j\omega\tau_{M,\alpha})^{\beta_2})^{\gamma_2}}, \tag{8}$$

where $\tau_{M,i}$ (i = σ,α) are relaxation times and $\Delta M_i = M_{S,i} - M_{\infty,i}$ amplitudes for the electric modulus. The subscripts S and ∞ stand for the limiting low and high frequency values of each process. β_i and γ_i are dimensionless parameters that control the shape of the relaxation ($0 < \beta \leq 1$, $\beta\gamma \leq 1$); the former describes the symmetric and the later the asymmetric broadening of the complex electric modulus in the same way as for the complex dielectric permittivity. All the above-mentioned parameters are temperature-dependent. As an example, in Figure 6 both components of the complex modulus as a

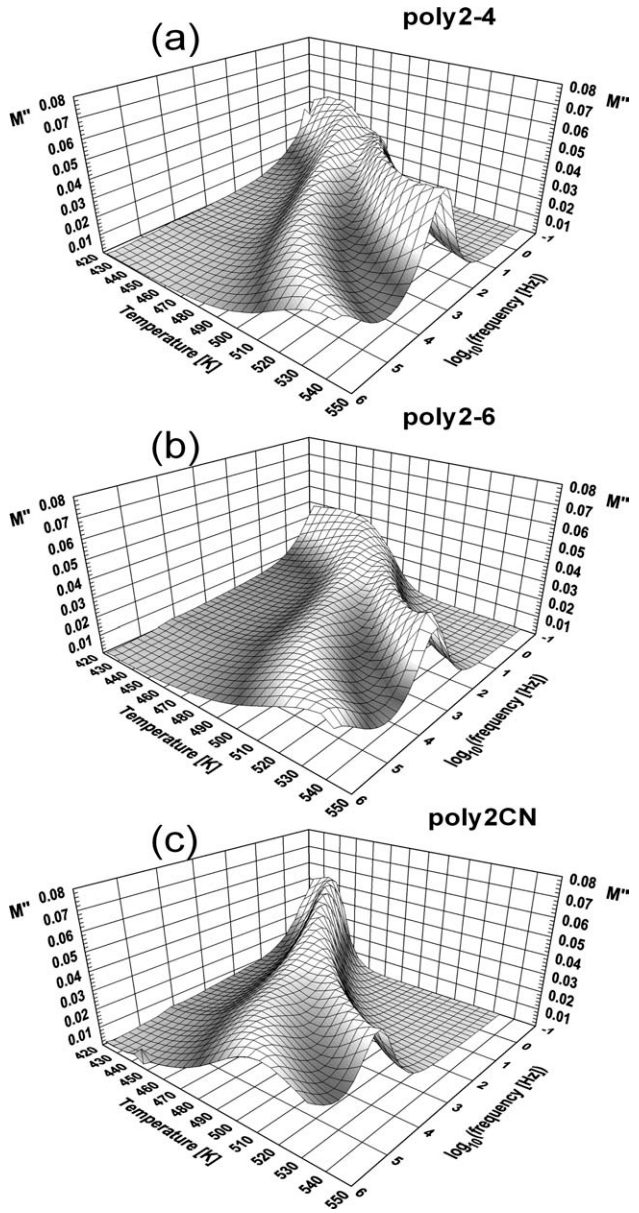

Figure 5 Three-dimensional plots of M'' versus frequency and temperature for a) poly2-4, b) poly2-6, and c) poly2CN.

function of the frequency for (a) poly2-4 at 513 K, (b) poly2-6 at 513 K and (c) poly2CN at 503 K, with their corresponding fittings are plotted. Figure 7 stands for the same temperatures but in this case we have represented M'' versus M' (Argand diagram). The solid line represents the best fit to eq. (8) (we fit both components simultaneously) and the dashed line the deconvolution into elementary modes α and σ. The shape of the conductivity contribution is near the Cole-Davidson function for all temperatures ($\beta_1 \approx 1$, $\gamma_1 \neq 1$) and narrower than the dipolar α relaxation for which both parameters are different from 1 as it is clearly evidenced in Figure 7; the arcs related with the dipolar relaxation are far from semicircles. As a trend, both parameters diminish with decreasing temperature being the shape of poly2CN the farthest from Debye.

Additional information can be extracted regarding the dipolar α relaxation from the fitted parameters. When the dielectric function ε*(ω) does not follow the Debye law (if it follows, for example, the

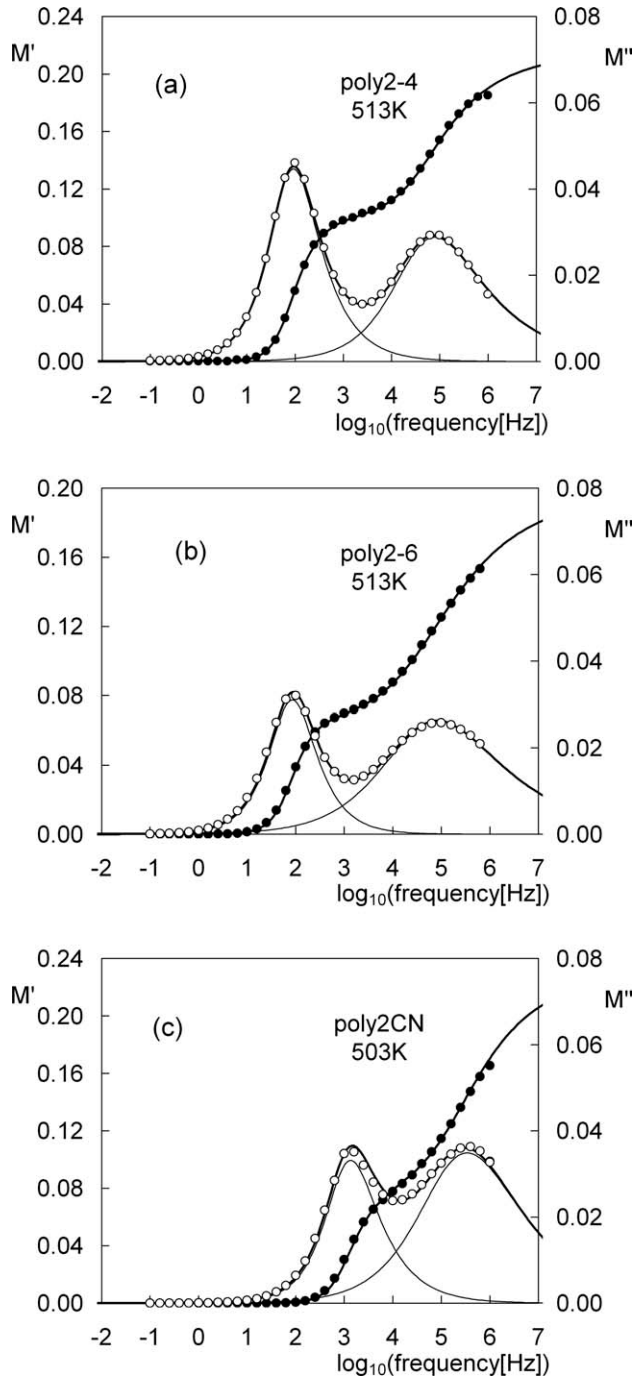

Figure 6 M' (full dots) and M'' (empty dots) versus frequency for a) poly2-4 at 513 K, b) poly2-6 at 513 K, and c) poly2CN at 503 K. Solid thick lines represent the best fit to eq. (8) and the thinner lines the deconvolution into elementary modes α (high frequency) and σ (low frequency).

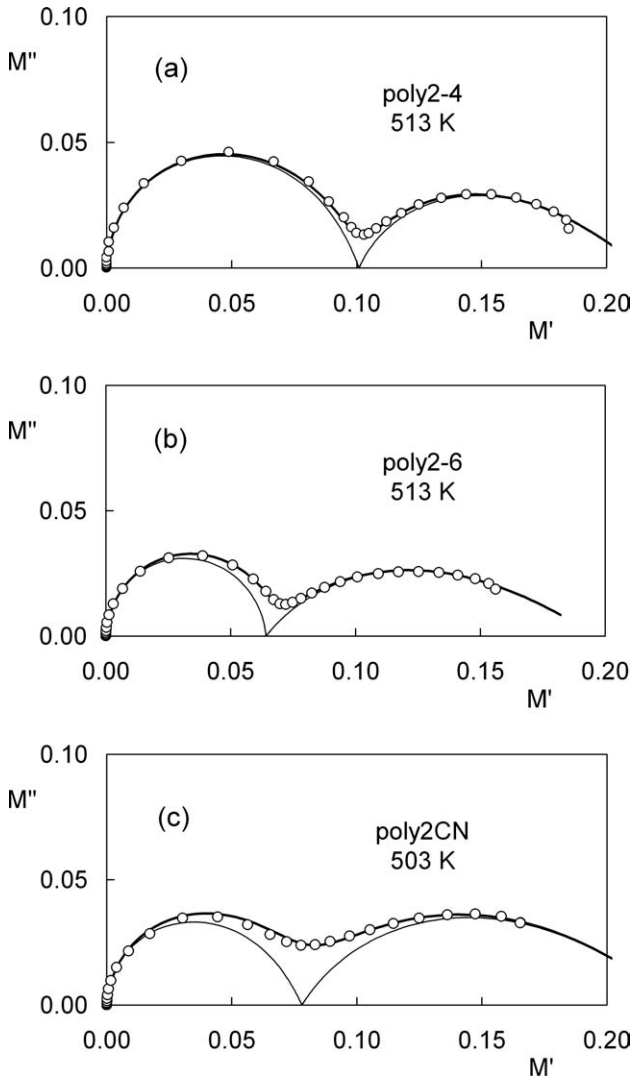

Figure 7 Argand diagram, M'' versus M' for a) poly2-4 at 513 K, b) poly2-6 at 513 K, and c) poly2CN at 503 K. Solid thick lines represent the best fit to eq. (8) and the thinner lines the deconvolution into elementary modes α (high frequency) and σ (low frequency).

Havriliak-Negami law) there is not a direct relationship between parameters[30] (relaxation times, shape parameters, etc), and still some information can be extracted. First, note that $M_\infty = 1/\varepsilon_\infty$ and $\Delta M_\alpha = 1/\varepsilon_{S,\alpha} - 1/\varepsilon_\infty$.[14,30] From this last expression one can deduce:

$$\Delta\varepsilon_{M,\alpha} = \frac{-\varepsilon_\infty^2 \Delta M_\alpha}{1 + \varepsilon_\infty \Delta M_\alpha}, \tag{9}$$

where we have labeled the dielectric strength of the mode related with α with the subscript M to indicate that this value was deduced from the fits of the electric modulus. On the other hand, we could also deduce approximate values for this dielectric strength assuming for ε_∞ the low frequency value of ε' at low temperature (room temperature in our case) and for $\varepsilon_{S,\alpha}$ the low frequency value of ε' at temperatures $T > T_g$, high enough to ensure that the dipoles could move freely. The values for ε_∞ (Table I) coincided quite well with those deduced from the fits of the modulus. To determine $\varepsilon_{S,\alpha}$, 10 Hz was chosen as the optimal frequency; for lower frequencies the conductivity contribution becomes very important. The values deduced in this way for the dipolar dielectric strength, $\Delta\varepsilon_{\varepsilon,\alpha}$, for all investigated polymers at temperature $(T_g + 45)$ K are shown in Table I, together with those deduced from M, $\Delta\varepsilon_{M,\alpha}$, at the same temperatures. It is evident that $\Delta\varepsilon_{\varepsilon,\alpha} > \Delta\varepsilon_{M,\alpha}$, an observation that should be expected because $\varepsilon_{S,\alpha}$ is overestimated due to the conductivity contribution. It is important to point out that most authors[5] obtain the dipolar dielectric strength the same way we deduced $\Delta\varepsilon_{\varepsilon,\alpha}$.

In Figure 8 (poly2-4), Figure 9 (poly2-6), and Figure 10 (poly2CN) we show an Arrhenius plot with frequencies of the maxima of M'' for the dipolar α process (empty dots) and conductivity process (empty squares). These frequencies are related to the relaxation times[19,31]:

$$f_{(\mathrm{HN})M,i} = \frac{1}{2\pi\tau_{M,i}}\left[\mathrm{sen}\frac{\beta_{M,i}\pi}{2+2\gamma_{M,i}}\right]^{1/\beta_{M,i}}\left[\mathrm{sen}\frac{\beta_{M,i}\gamma_{M,i}\pi}{2+2\gamma_{M,i}}\right]^{-1/\beta_{M,i}}, \tag{10}$$

where HN stands for Havriliak-Negami. Both sets of frequencies can be fitted into the Vogel-Fulcher-Tamman law (VFT) above the glass transition, T_g (calorimetric glass transition temperature)[32]:

$$f_{(\mathrm{HN})M,i} = f_{0,i}\exp\left(\frac{A_{M,i}}{T - T_{0,i}}\right), \tag{11}$$

$f_{0,i}$ and $A_{M,i}$ are empiric constants and $T_{0,i}$ is the so-called ideal glass transition temperature or Vogel temperature. The best-fit values of these parameters are presented in Table II. $T_{0,i}$ values are different for the conductivity and dipolar processes for the three compounds, being higher for the α process than for the σ process. These results could indicate that the dipole mobility is suppressed at higher temperatures

TABLE I
Dielectric Strength of the α Dipolar Process Deduced from the Electric Modulus, $\Delta\varepsilon_{M,\alpha}$, See Text, and from the Measurements of the Permittivity at 10 Hz $\Delta\varepsilon_{\varepsilon,\alpha}$ and the High-Frequency Permittivity ε_∞

	$\Delta\varepsilon_{\varepsilon,\alpha}$	$\Delta\varepsilon_{M,\alpha}$	ε_∞
Poly2-4	7.0	4.9	4.6
Poly2-6	11.8	9.6	4.8
Poly2cn	15.9	12.5	4.5

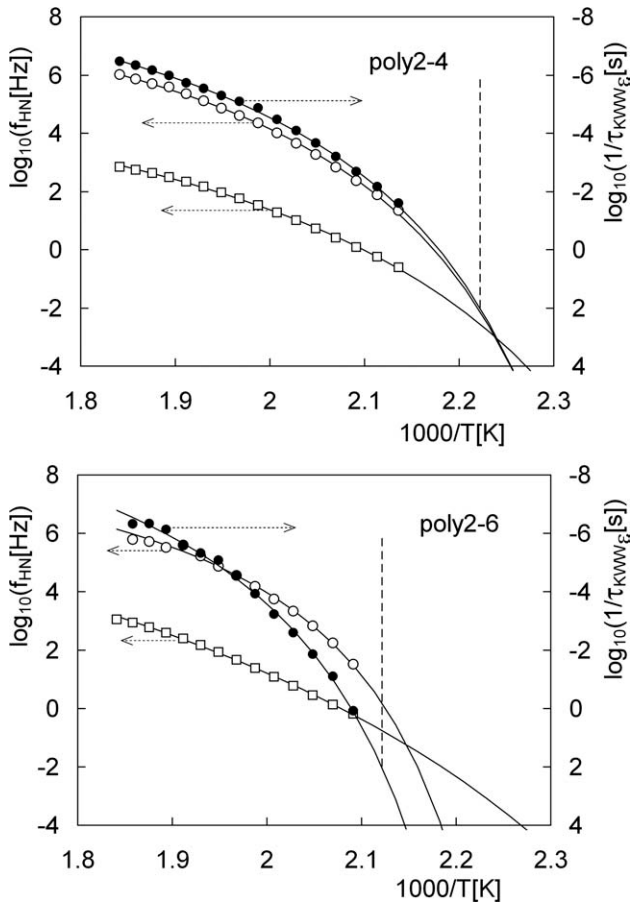

Figure 8 Arrhenius plot of $f_{HN,}$ frequency of the maximum of M″, as deduced from the fits of the electric modulus to eq. (8) for the α dipolar process, empty circles, and for the σ process, empty squares. Full circles, scale on the right, are the relaxation times associated to a KWW behavior of the dielectric permittivity for the α process [see text, eqs. (10)–(15)]. Solid lines are fits to the VFT law; parameters are listed in Table II (a, poly2-4, b, poly2-6).

than the mobility of the charge carriers that are responsible for the conductivity

Before further explaining the parameters in Table II we will clarify how we proceeded to obtain more insights regarding the "dielectric" behavior of the dipolar α process. As we have mentioned, a HN shape for the modulus does not means a HN for the permittivity,[19] and for example there is not a direct relationship between the frequencies of the maxima (*id.* relaxation times) of both M'' and ε''. First, as mentioned above, from the fits of the modulus one can obtain $\tau_{M,\alpha}$. To simplify the notation we called this relaxation time $\tau_{(HN)M}$ because we will only deal with the dipolar process. Under certain approximations one can relate the HN shape with the Kohlrausch-Williams-Watts (KWW) shape, leading to a relationship between the corresponding relaxation times[33]:

$$\log_{10}\frac{\tau_{(NH)M}}{\tau_{(KWW)M}} \approx 2.6(1-n_M)^{0.5}\exp(-3n_M), \qquad (12)$$

where the n_M index is the index of the stretched exponential representing the KWW function and is related to the parameters of the HN function:

$$\beta_{(HN)M}\gamma_{(HN)M} = n_M^{1.23}, \qquad (13)$$

whenever the HN parameters range under certain limits. These approaches require $\alpha > 0.4$ and $\gamma > 0.2$, which was always our case. Then, assuming a KWW shape for the modulus, the dielectric permittivity should have also a KWW shape and the following expressions can be used to relate $\tau_{(KWW)M}$ and $\tau_{(KWW)\varepsilon}$[30]:

$$\tau_{(KWW)M} = \left(\frac{\varepsilon_\infty}{\varepsilon_S}\right)^{1/n_\varepsilon}\tau_{(KWW)\varepsilon}, \qquad (14a)$$

$$\tau_{(KWW)\varepsilon} = \left(\frac{M_S}{M_\infty}\right)^{1/n_M}\tau_{(KWW)M}, \qquad (14b)$$

where $n_M \approx 0.8n_\varepsilon$. This procedure has been used only for poly2-4 and poly2-6; for poly2CN, due to the larger conductivity contribution, the fits for the dipolar process, although good enough for the frequency of the modulus, have some dispersion for the shape parameters and then in the relaxation times. For poly2-4 and poly2-6 β ranges between 0.75 and 0.50 and γ between 0.65 and 0.30. The obtained values for $\tau_{(KWW)\varepsilon}$ have been also represented in Figure 8 (full dots) and 9 (full dots) and fitted to the VFT law:

$$\tau_{(KWW)\varepsilon} = \tau_0 \exp\left(\frac{DT_{0,\alpha}}{T - T_{0,\alpha}}\right) \qquad (15)$$

where D, strength parameter, is such that DT_0 has the same role as A in eq. (11). The $T_{0,\alpha}$ value

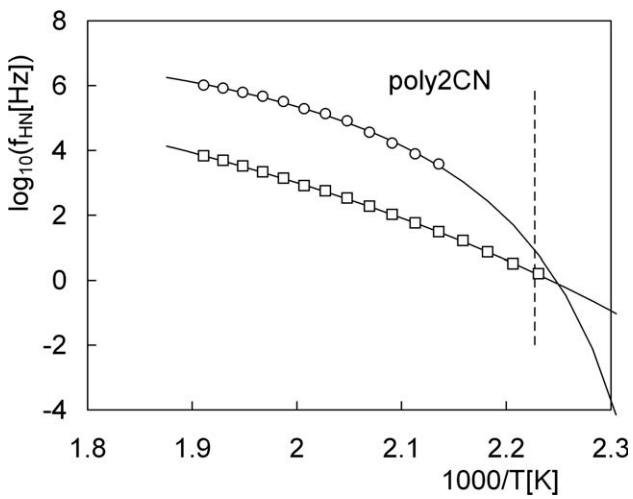

Figure 9 Arrhenius plot of f_{HN}, frequency of the maximum of M'', as deduced from the fits of the electric modulus to eq. (8) for the α dipolar process, empty circles, and for the σ process, empty squares.

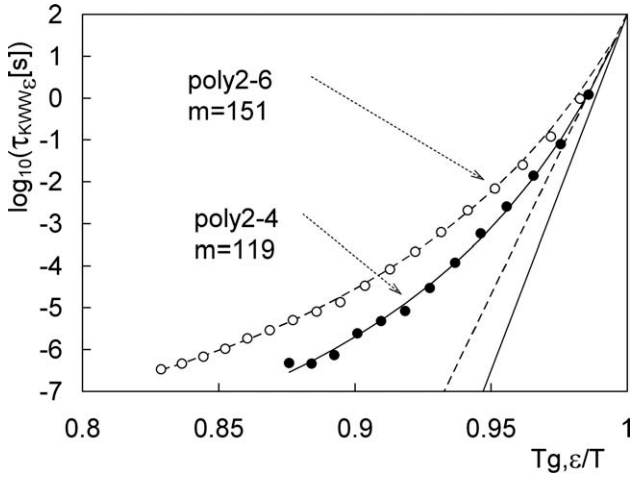

Figure 10 Angell plot of the relaxation times associated to a KWW behavior of the dielectric permittivity for the α process [see text, eqs. (10)–(15)] for poly2-4 (full circles) and poly2-6 (empty circles) together with the fits to the VFT law and slopes at $T = T_{g,\varepsilon}$. Continuous lines correspond to poly2-4 and dashed lines to poly2-6.

obtained from this fit is the same as the obtained from the fit of the frequency of the maxima of the imaginary part of the modulus, which allowed us to be confident about the procedure. From this fit we have also deduced the dielectric glass transition temperature, $T_{g,\varepsilon}$, as the value for which the relaxation time $\tau_{(KWW)\varepsilon}$, (τ_ε further on) reached the value 10^2 s. This temperature was slightly lower than the calorimetric one for poly2-6, 19 K lower for poly2-4 and in both cases were between 40 and 50 K higher than the corresponding Vogel temperature. We have introduced concepts such as "fragility" to understand how and why these relaxation times (associated with the α process and then related to the glass transition) show such an increase as predicted by the VFT in a short temperature range. The idea was to analyze how far from an Arrhenius behavior is the temperature dependence of the relaxation time. Fragility, dynamic fragility, can be quantified in various ways, for example, by using D, the strength parameter. The more fragile the material, the lesser the strength parameter. Values of D lower than 10 imply larger deviations from the Arrhenius law and the materials are denoted as fragile. In our case, it took values of 3.65 and 3.40 for poly2-4 and poly2-6, respectively. Another way to evaluate the fragility is through the fragility index, m, defined as[34,35]:

$$m = \left[\frac{d(\log_{10}\tau_\varepsilon)}{d(T_{g,\varepsilon}/T)}\right]_{T=T_{g,\varepsilon}}, \tag{16}$$

m accounts for the slope at $T_{g,\varepsilon}$ in an Angell plot ($\log_{10}\tau_\varepsilon$ vs. $T_{g,\varepsilon}/T$), see Figure 10. Dashed (poly2-6) and continuous (poly2-4) lines are fits to the VFT law, eq. (15), with each respective slope at $T_{g,\varepsilon}$ that allow to deduce m as:

$$m = \frac{DT_{0,\alpha}}{2.3(1 - T_{0,\alpha}/T_{g,\varepsilon})^2}. \tag{17}$$

In our case, we obtained 119 for poly2-4 and 151 for poly2-6. The lower limit of m is assigned to 16, the strongest materials.[35,36] On the other hand, the most fragile glass-forming materials have values of m up to 200 or even more. In general, polymers exhibit higher fragility than nonpolymeric glass-forming systems, being the chain rigidity one of the main reasons of this behavior. Our values are relatively high. This fact could be related to the high value of the glass transition temperatures and high chain rigidity.[37]

Thermally stimulated depolarization current (TSDC) measurements

The $\Delta\varepsilon_{M,\alpha}$ values deduced from eq. (9) have been used to determine from eq. (1) the frozen-in polarization values, $P_{r,M}$, for the three polyimides (we use the subscripts to indicate that the dielectric strength has been deduced from the modulus). These values are recovered in Table III. However, P_r can be directly obtained from TSDC measurements by integrating the depolarization current, $i(T)$, eq. (3). This depolarization current was measured for the three polyimides polarized at conditions stated in the experimental part. Although this study has been partially published previously,[10,38] for completeness we include the results.

The maxima of the depolarization current appear at temperatures T_m corresponding to the maximum mobility of the molecules. The T_m values are 468, 476, and 457 K for poly2-4, poly2-6, and poly2CN, respectively. The lowest T_m, and also T_g, are obtained for poly2CN owing to its larger number of ether groups in the repetitive unit that increases the molecular flexibility of the polymer. Above the depolarization peak, the value of the current increases sharply. This behavior is directly associated to the increase of the conductivity for temperatures above T_g for the three polymers. This effect is particularly relevant for poly2CN, which is in accordance with the dielectric permittivity

TABLE II
Parameters Deduced from the Fits to the VFT Law

	$T_{0,\sigma}$ (K)	$A_{M,\sigma}$ (K)	$T_{0,\alpha}$ (K)	$A_{M,\alpha}$ (K)	T_g (K)	$T_{g,\varepsilon}$ (K)	$DT_{0,\alpha}$ (K)	m
Poly2-4	373.7	1745	401	1401	469	450	1462	119
Poly2-6	332.3	3683	427	983	473	471.4	1452	151
Poly2cn	306.6	3450	410.6	684	449			

TABLE III
Parameters Related with eq. (18)

	ρ (kg·m^{-3})	$M_{monomer}$ (kg·mol^{-1})	$P_{\gamma,M}$ (mC·m^{-2})	P_γ(TSDC) (mC·m^{-2})	$\mu_0 \langle \cos \theta \rangle$ (D)
Poly2-4	1348	0.5914	1.5	1.6 ± 0.1	0.15
Poly2-6	1357	0.5914	3.0	3.1 ± 0.3	0.29
Poly2cn	1405	0.8005	3.9	4.3 ± 0.4	0.51

measurements (Fig. 2). The integrated P_r values at room temperature for the three polyimides are listed in Table III. These values are in very good agreement with the $P_{r,M}$ obtained from eq. (1). The consistency of these results indicates that the polarization of these polymers films arise from orientational polarization and not from space charges.

The relative values of this magnitude could be interpreted on the basis of the chemical structure of the repetitive units of each polyimide. These structures, together with the most important dipolar moments and possible axis of torsional rotation of molecular segments,[4] are shown in Figure 1. Poly2-6 and poly2-4 have one dipolar CN group but in a different position, whereas poly2CN has two. Using the Mopsik-Broadhurst model[39] the value of the frozen-in polarization of amorphous molecular dipole electrets is given by:

$$P_r = \frac{N}{3V}(\varepsilon_\infty + 2)\mu_0\langle\cos\theta\rangle, \qquad (18)$$

where N/V is the number of dipoles per unit volume and θ is the angle between the poling direction, perpendicular to the surface of the polymer film, and the dipole axis, being $\mu_0 \langle \cos \theta \rangle$ the average value of the permanent dipole moment of the monomer along the poling direction. Knowing the density, the monomer mass, and ε_0, shown in Tables I and III, $\mu_0 \langle \cos \theta \rangle$ was calculated (also listed in Table III). Park et al.[5] and Young et al.[4] have shown that for poly2-6, an increase of the degree of imidization induces a decrease of the mobility of the dipoles in the polymer chain, being the *N*-phenyl phthalimide groups especially affected by this phenomenon. The fully cured imide form of the polymer does not have independently polarizable fragments.[5] The frozen-in polarization of totally cured and poled at the same condition as poly2-6 polymer APB/ODPA films[38] (similar repetitive unit but without pendant dipolar CN groups) is 0.14 mC/m^2. It makes less than 5% of the total polarization value of poly2-6 films. These results allow us to suppose that in totally cured films of poly2-6 the dominant part of the frozen-in polarization is directly related to the CN pendant group orientation.

According to the molecular modeling of the poling of polyimides suggested by Young et al.,[4] the frozen-in polarization of poly2-6 poled at E_p = 150 MV/m should be around 24 mC/m^2 with 48% of the total polarization being due to the nitrile substituent and 39% due to the anhydride residues. Taking into consideration the results of the above model and eqs. (1) and (18), one can obtain a value for $\mu_0 <\cos \theta>$ of around 0.26 D, which is in very good agreement with the value calculated for poly2-6 from TSDC measurements (see Table III) and confirms that, in totally cured samples, 90% of the polarization is due to the orientation of the dipolar CN groups. The values of $\mu_0 <\cos \theta>$ for poly2-4 and poly2CN are also consistent with the chemical structure of their corresponding monomers. In the case of poly2-4, its value is half that of poly2-6, as it could be expected because of the different position of the CN group in the aromatic ring. On the other hand, its value for poly2CN relative to poly2-6 is not the double as a result of steric effects limiting the orientation of the CN groups in the electric field.

CONCLUSIONS

Here, we have studied the effect of the number and position in the aromatic rings of the dipolar CN groups on the dielectric properties and frozen-in polarization of three amorphous polyimides. Using the electric modulus formalism to analyze the dielectric response at temperatures above the glass transition temperature, we have been able to discriminate between dipolar and conductive contributions. We have evaluated the dielectric dipolar strength associated with the α dipolar process and the corresponding relaxation time. We followed several steps that involve relationships between the modulus and the permittivity, and also between relaxation shapes, NH versus KWW. The obtained relaxation time, associated to the permittivity, shape KWW, follows the VFT law. From its temperature dependence we have obtained the fragility index. Resulting values are quite high, indicating that the polyimides under study are very fragile.

A comparison of the frozen-in polarization values obtained by means of the thermally stimulated depolarization current method (TSDC) and those calculated from the dielectric strength allows us to conclude that in totally cured samples the frozen-in polarization is due mainly to the dipole orientation of the dipolar CN groups and depends on the number of groups and on their position in the aromatic rings.

So, we can conclude that, to optimize (increase) the frozen-in polarization, the strategy could be to increase the number of CN pedant groups in the monomer and modify the curing process to activate the *N*-phenyl phthalimide groups in the orientational polarization process. Also, the use of different anhydrides with polar groups could enhance the piezoelectric response.

References

1. Wu, S. L.; Scheinbein, J. I.; Newman, B. A. J Polym Sci Part B: Polym Lett 1999, 37, 2737.
2. Giacometti, J. A.; De Reggi, A. S.; Davis, G.; Thomas, D.; Brian, F.; Leal, G. F. J Appl Phys 1996, 80, 6407.
3. Tasaka, S.; Toyama, T.; Inagaki, N. Jpn J Appl Phys 1994, 33, 5838.
4. Young, J. A.; Farmer, B. L.; Hinkley, J. A. Polymer 1999, 40, 2787.
5. Park, C.; Ounaies, Z.; Wise, K. E.; Harrison, J. S. Polymer 2004, 45, 5417.
6. Mittal, K. L. Polyimides and Other High Temperature Polymers: Synthesis, Characterization and Applications; VSP Publication: Netherland, 2009; Vol.5, p. 213.
7. Licari, J. J. Coating Materials for Electronic Applications; Elsevier: USA, 2003, p. 32.
8. Bauer, S.; Lang, S. B. IEEE Trans Dielectrics Electrical Insulation 1996, 3, 647.
9. Hinkley, J. A. High Perform Polym 1996, 8, 427.
10. Gonzalo, B.; Vilas, J. L.; Breczewski, T.; Pérez-Jubindo, M. A.; de la Fuente, M. R.; Rodríguez, M.; León, L. M. J Polym Sci Part A: Polym Chem 2009, 47, 722.
11. Migahed, M. D.; Ahmed, M. T.; Kotp, A. E. J Macromol Sci Phys 2005, 44, 43.
12. Qu, W.; Ko, T.; Vora, R. H.; Chung, T. Polymer 2001, 42, 6393.
13. Schönhals, A. In Broadband Dielectric Spectroscopy; Kremer, F., Schönhals, A., Eds.; Springer-Verlag: Berlin, 2003, p.242.
14. Kramarenko, W. Y.; Ezquerra, T. A.; Privalko, V. P. Phys Rev E: Stat Phys Plasmas Fluids Relat 2003, 67, 031801/1.
15. Moynihan, C. T.; Bressel, R. D.; Angell, C. A. J Chem Phys 1971, 55, 4414.
16. Elliott, S. R. J Non-Cryst Solids 1994, 172, 1343.
17. Jonscher, A. K. Nature 1977, 267, 673.
18. Macedo, P. B.; Moynihan, C. T.; Bose, R. Phys Chem Glasses 1972, 13, 171.
19. Schönhals, A.; Kremer, F. In Broadband Dielectric Spectroscopy; Kremer, F., Schönhals, A., Eds.; Springer-Verlag: Berlin, 2003, p. 35.
20. McCrum, N. G.; Read, B. E.; Eilliams, G. In Anelastic and Dielectric Effects in Polymeric Solids; Wiley: New York, 1991, p. 57.
21. Neagu, E.; Pissis, P.; Apekis, L.; Gomez-Ribelles, J. L. J Phys D: Appl Phys 1997, 30, 1551.
22. Neagu, E.; Pissis, P.; Apekis, L. J Appl Phys 2000, 87, 2914.
23. Neagu, R. M.; Neagu, E.; Kyritsis, A.; Pissis, P. J Phys D: Appl Phys 2000, 33, 1921.
24. Neagu, R. M.; Neagu, E.; Kyritsis, A.; Pissis, P. J Appl Phys 2000, 88, 6669.
25. Diaz Calleja, R.; Friederichs, S.; Jaimes, C.; Sanchis, J. M.; Belana, J.; Canadas, J. C.; Diego, J. A.; Mudarra, M. Polym Int 1998, 46, 20.
26. Kanapitsas, A.; Pissis, P.; Gómez-Ribelles, J. L.; Monleón-Pradas, M.; Privalko, E. G.; Privalko, V. P. J Appl Polym Sci 1999, 71, 1209.
27. Georgoussis, G.; Kyritsis, A.; Bershtein, V. A.; Fainleib, A. M.; Pissis, P. J Polym Sci Part B: Polym Phys 2000, 38, 3070.
28. Shilov, V. V.; Shevchenko, V. V.; Pissis, P.; Kyritsis, A.; Georoussis, G.; Gomza, Y. P.; Nesin, S. D.; Klimenko, N. S. J Non-Cryst Solids 2000, 275, 116.
29. Havriliak, S.; Negami, S. Polymer 1967, 8, 161.
30. Wagner, H.; Richert, R. Polymer 1997, 38, 255.
31. Díaz-Calleja, R. Macromolecules 2000, 33, 8924.
32. Powles, J. G.; Williams, M. L.; Evans, W. Mol Phys 1989, 66, 1107.
33. Álvarez, F.; Alegria, A.; Colmenero, J. Phys Rev B: Solid State 1993, 47, 125.
34. Böhmer, R.; Ngai, K. L.; Angell, C. A.; Plazek, D. J. J Chem Phys 1993, 99, 4201.
35. Böhmer, R.; Angell, C. A. Phys Rev B: Solid State 1992, 45, 10091.
36. Salud, J.; López, D. O.; Diez-Berart, S.; Pérez-Jubindo, M. A.; de la Fuente, M. R.; Rute, M. A.; Puertas, R. J Non-Cryst Solids 2009, 355, 2550.
37. Sokolov, A. P.; Novikov, V. N.; Ding, Y. J Phys Condens Matter 2007, 19, 205116.
38. San Sebastian, M.; Gonzalo, B.; Breczewski, T.; Vilas, J. L.; Pérez-Jubindo, M. A.; de la Fuente, M. R.; Rodriguez, M.; León, L. M. Ferroelectrics 2009, 389, 114.
39. Mopsik, F. I.; Broadhurst, M. G. J Appl Phys 1975, 46, 4204.